

Large-Scale Image Geo-Localization Using Dominant Sets

Eyasu Zemene^{ib}, *Student Member, IEEE*, Yonatan Tariku Tesfaye^{ib}, *Student Member, IEEE*,
Haroon Idrees, *Member, IEEE*, Andrea Prati^{ib}, *Senior Member, IEEE*,
Marcello Pelillo^{ib}, *Fellow, IEEE*, and Mubarak Shah^{ib}, *Fellow, IEEE*

Abstract—This paper presents a new approach for the challenging problem of geo-localization using image matching in a structured database of city-wide reference images with known GPS coordinates. We cast the geo-localization as a clustering problem of local image features. Akin to existing approaches to the problem, our framework builds on low-level features which allow local matching between images. For each local feature in the query image, we find its approximate nearest neighbors in the reference set. Next, we cluster the features from reference images using Dominant Set clustering, which affords several advantages over existing approaches. First, it permits variable number of nodes in the cluster, which we use to dynamically select the number of nearest neighbors for each query feature based on its discrimination value. Second, this approach is several orders of magnitude faster than existing approaches. Thus, we obtain multiple clusters (different local maximizers) and obtain a robust final solution to the problem using multiple weak solutions through constrained Dominant Set clustering on global image features, where we enforce the constraint that the query image must be included in the cluster. This second level of clustering also bypasses heuristic approaches to voting and selecting the reference image that matches to the query. We evaluate the proposed framework on an existing dataset of 102k street view images as well as a new larger dataset of 300k images, and show that it outperforms the state-of-the-art by 20 and 7 percent, respectively, on the two datasets.

Index Terms—Geo-localization, dominant set clustering, multiple nearest neighbor feature matching, constrained dominant set

1 INTRODUCTION

IMAGE geo-localization, the problem of determining the location of an image using just the visual information, is remarkably difficult. Nonetheless, images often contain useful visual and contextual informative cues which allow us to determine the location of an image with variable confidence. The foremost of these cues are landmarks, architectural details, building textures and colors, in addition to road markings and surrounding vegetation.

Following the recent outstanding advances in the area of image matching, geo-localization approaches based on it

has attracted a lots of interest in computer vision community [1], [2], [3], [4]. In [1], the authors find the first nearest neighbor (NN) for each local feature in the query image, prune outliers and use a heuristic voting scheme for selecting the matched reference image. The follow-up work [2] relaxes the restriction of using only the first NN and proposed Generalized Minimum Clique Problem (GMCP) formulation for solving this problem. However, GMCP formulation can only handle a fixed number of nearest neighbors for each query feature. The authors used 5 NN, and found that increasing the number of NN drops the performance. Additionally, the GMCP formulation selects exactly one NN per query feature. This makes the optimization sensitive to outliers, since it is possible that none of the 5 NN is correct. Once the best NN is selected for each query feature, a very simple voting scheme is used to select the best match. Effectively, each query feature votes for a single reference image, from which the NN was selected for that particular query feature. This often results in identical number of votes for several images from the reference set. Then, both [1], [2] proceed with randomly selecting one reference image as the correct match to infer GPS location of the query image. Furthermore, the GMCP is a binary-variable NP-hard problem, and due to the high computational cost, only a single local minima solution is computed in [2].

In this paper, we propose an approach to image geo-localization by robustly finding a matching reference image to a given query image. This is done by finding correspondences between local features of the query and reference images. We first introduce automatic NN selection into our

- E. Zemene is with DAIS, Ca' Foscari University of Venice, Venezia, VE 30123, Italy and Center for Research in Computer Vision (CRCV), University of Central Florida, Orlando, FL 32816. E-mail: eyasu.zemene@unive.it.
- Y. Tariku Tesfaye is with the Department of Design and Planning in Complex Environments of the University IUAV of Venice, Venezia, VE 30135, Italy and Center for Research in Computer Vision (CRCV), University of Central Florida, Orlando, FL 32816. E-mail: y.tesfaye@stud.iuav.it.
- A. Prati is with the Department of Engineering and Architecture of the University of Parma, Parma, PR 43121, Italy. E-mail: andrea.prati@unipr.it.
- M. Pelillo is with DAIS, Ca' Foscari University of Venice, Venezia, VE 30123, Italy. E-mail: pelillo@unive.it.
- H. Idrees and M. Shah are with the Center for Research in Computer Vision (CRCV), University of Central Florida, Orlando, FL 32816. E-mail: {haroon, shah}@eecs.ucf.edu.

Manuscript received 15 Jan. 2017; revised 13 Nov. 2017; accepted 8 Dec. 2017. Date of publication 31 Dec. 2017; date of current version 12 Dec. 2018.

(Corresponding author: Eyasu Zemene Mequanint.)

Recommended for acceptance by J. Sivic.

For information on obtaining reprints of this article, please send e-mail to: reprints@ieee.org, and reference the Digital Object Identifier below.

Digital Object Identifier no. 10.1109/TPAMI.2017.2787132

framework, by exploiting the discriminative power of each NN feature and employing different number of NN for each query feature. This also bypasses the manual tuning of the number of NNs to be considered, which can vary between datasets and is not straightforward.

Our approach to image geo-localization is based on *Dominant Set clustering* (DSC)—a well-known generalization of maximal clique problem to edge-weighted graphs—where the goal is to extract the most compact and coherent set. It's intriguing connections to evolutionary game theory allow us to use efficient game dynamics, such as replicator dynamics and infection-immunization dynamics (InImDyn). InImDyn has been shown to have a linear time/space complexity for solving standard quadratic programs (StQPs), programs which deal with finding the extrema of a quadratic polynomial over the standard simplex [5], [6].

The proposed approach is on average 200 times faster and yields an improvement of 20 percent in the accuracy of geo-localization compared to [1], [2]. Furthermore, our solution uses a linear relaxation to the binary variables, which in the absence of hard constraints is solved through an iterative algorithm resulting in massive speed up.

Since the dynamics and linear relaxation of binary variables allow our method to be extremely fast, we run it multiple times to obtain several local maxima as solutions. Next, we use a query-based variation of DSC to combine those solutions to obtain a final robust solution. The query-based DSC uses the soft-constraint that the query, or a group of queries, must always become part of the cluster, thus ensuring their membership in the solution. We use a fusion of several global features to compute the cost between query and reference images selected from the previous step. The members of the cluster from the reference set are used to find the geo-location of the query image. Note that, the GPS location of matching reference image is also used as a cost in addition to visual features to ensure both visual similarity and geographical proximity.

GPS tagged reference image databases collected from user uploaded images on Flickr have been typically used for the geo-localization task. The query images in our experiments have been collected from Flickr, however, the reference images were collected from Google Street View. The data collected through Flickr and Google Street View differ in several important aspects: the images downloaded from Flickr are often redundant and repetitive, where images of a particular building, landmark or street are captured multiple times by different users. Typically, popular or tourist spots have relatively more images in testing and reference sets compared to less interesting parts of the urban environment. An important constraint during evaluation is that the distribution of testing images should be similar to that of reference images. On the contrary, Google Street View reference data used in this paper contains only a single sample of each location of the city. However, Street View does provide spherical 360 degree panoramic views, approximately 12 meters apart, of most streets and roads. Thus, the images are uniformly distributed over different locations, independent of their popularity. The comprehensiveness of the data ensures that a correct match exists; nonetheless, at the same time, the sparsity or uniform distribution of the data makes geo-localization difficult, since

every location is captured in only few of the reference images. The difficulty is compounded by the distorted, low-quality nature of the images as well.

The main contributions of this paper are the following:

- We present a robust and computationally efficient approach for the problem of large-scale image geo-localization by locating images in a database of city-wide reference images with known GPS coordinates.
- We formulate geo-localization problem in terms of a more generalized form of dominant sets framework which incorporates weights from the nodes in addition to edges.
- We take a two-step approach to solve the problem. The first step uses local features to find putative set of reference images (and is therefore faster), whereas the second step uses global features and a constrained variation of dominant sets to refine results from the first step, thereby, significantly boosting the geo-localization performance.
- We have collected new and more challenging high resolution reference dataset (**WorldCities** dataset) of 300K Google street view images.

The rest of the paper is structured as follows. We present literature relevant to our problem in Section 2, followed by technical details of the proposed approach in Section 3, while constrained dominant set based post processing step is discussed in Section 4. This is followed by dataset description in Section 5.1. Finally, we provide results of our extensive evaluation in Section 5 and conclude in Section 6.

2 RELATED WORK

The computer vision literature on the problem of geo-localization can be divided into three categories depending on the scale of the datasets used: landmarks or buildings [7], [8], [9], [10], city-scale including streetview data [11], and worldwide [3], [12], [13]. Landmark recognition is typically formulated as an image retrieval problem [7], [9], [10]. For geo-localization of landmarks and buildings, Crandall et al. [14] perform structural analysis in the form of spatial distribution of millions of geo-tagged photos. This is used in conjunction with visual and meta data from images to geo-locate them. The datasets for this category contain many images near prominent landmarks or images. Therefore, in many works [7], [9], similar looking images belonging to same landmarks are often grouped before geo-localization is undertaken.

For citywide geo-localization of query images, Zamir and Shah [1] performed matching using SIFT features, where each feature votes for a reference image. The vote map is then smoothed geo-spatially and the peak in the vote map is selected as the location of the query image. They also compute 'confidence of localization' using the Kurtosis measure as it quantifies the peakiness of vote map distribution. The extension of this work in [2] formulates the geo-localization as a clique-finding problem where the authors relax the constraint of using only one nearest neighbor per query feature. The best match for each query feature is then solved using Generalized Minimum Clique Graphs, so that a simultaneous solution is obtained for all query features in contrast to their previous work [1]. In similar vein, Schindler

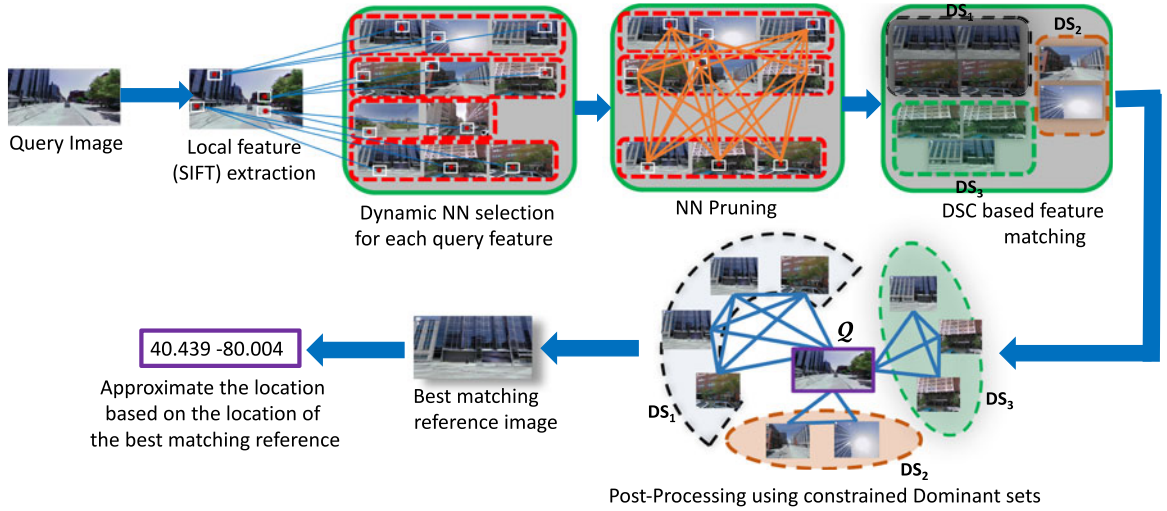


Fig. 1. For each query feature, we dynamically select NNs and remove query features which are less informative, we build fully connected graph between selected NN and extract candidate matching reference images using Dominant set clustering (DSC). Finally, we employ constrained dominant sets (CDS) based post processing to select best matching reference image and finally we approximate the location of the query based of the location of the best matching reference image.

et al. [4] used a dataset of 30,000 images corresponding to 20 kilometers of street-side data captured through a vehicle using vocabulary tree. Sattler et al. [15] investigated ways to explicitly handle geometric bursts by analyzing the geometric relations between the different database images retrieved by a query. Arandjelovic et al. [16] developed a convolutional neural network architecture for place recognition that aggregates mid-level (conv5) convolutional features extracted from the entire image into a compact single vector representation amenable to efficient indexing. Torii et al. [17] exploited repetitive structure for visual place recognition, by robustly detecting repeated image structures and a simple modification of weights in the bag-of-visual-word model. Zeisl et al. [18] proposed a voting-based pose estimation strategy that exhibits linear complexity in the number of matches and thus facilitates to consider much more matches.

For geo-localization at the global scale, Hays and Efros [3] were the first to extract coarse geographical location of query images using Flickr collected across the world. Recently, Weyand et al. [13] pose the problem of geo-locating images in terms of classification by subdividing the surface of the earth into thousands of multi-scale geographic cells, and train a deep network using millions of geo-tagged images. In the regions where the coverage of photos is dense, structure-from-motion reconstruction is used for matching query images [19], [20], [21]. Since the difficulty of the problem increases as we move from landmarks to city-scale and finally to worldwide, the performance also drops. There are many interesting variations to the geo-localization problem as well. Sequential information such as chronological order of photos was used by [22] to geo-locate photos. Similarly, there are methods to find trajectory of a moving camera by geo-locating video frames using Bayesian Smoothing [23] or geometric constraints [24]. Chen and Grauman [25] present Hidden Markov Model approach to match sets of images with sets in the database for location estimation. Lin et al. [26] use aerial imagery in conjunction with ground images for geo-localization. Others [27], [28] approach the problem by matching ground images against a database of aerial

images. Jacob et al. [29] geo-localize a webcam by correlating its video-stream with satellite weather maps over the same time period. Skyline2GPS [30] uses street view data and segments the skyline in an image captured by an upward-facing camera by matching it against a 3D model of the city.

Feature discriminativity has been explored by [31], who use local density of descriptor space as a measure of descriptor distinctiveness, i.e., descriptors which are in a densely populated region of the descriptor space are deemed to be less distinctive. Similarly, Bergamo et al. [32] leverage Structure from Motion to learn discriminative codebooks for recognition of landmarks. In contrast, Cao and Snavely [33] build a graph over the image database, and learn local discriminative models over the graph, which are used for ranking images according to the query. Similarly, Gronat et al. [34] train discriminative classifier for each landmark and calibrate them afterwards using statistical significance measures. Instead of exploiting discriminativity, some works use similarity of features to detect repetitive structures to find locations of images. For instance, Torii et al. [17] consider a similar idea and find repetitive patterns among features to place recognition. Similarly, Hao et al. [35] incorporate geometry between low-level features, termed 'visual phrases', to improve the performance on landmark recognition.

Our work is situated in the middle category, where given a database of images from a city or a group of cities, we aim to find the location where a test image was taken from. Unlike landmark recognition methods, the query image may or may not contain landmarks or prominent buildings. Similarly, in contrast to methods employing reference images from around the globe, the street view data exclusively contains man-made structures and rarely natural scenes like mountains, waterfalls or beaches.

3 IMAGE MATCHING BASED GEO-LOCALIZATION

Fig. 1 depicts the overview of the proposed approach. Given a set of reference images, e.g., taken from Google Street View, we extract local features (hereinafter referred as

reference features) using SIFT from each reference image. We then organize them in a k-means tree [36].

First, for each local feature extracted from the query image (hereinafter referred as *query feature*), we dynamically collect nearest neighbors based on how distinctive the two nearest neighbors are relative to their corresponding query feature. Then, we remove query features, along with their corresponding reference features, if the ratio of the distance between the first and the last nearest neighbor is too large (Section 3.1). This means that the query feature is not very informative for geo-localization, and is not worth keeping for further processing. In the next step, we formalize the problem of finding matching reference features to query features as a DSC (Dominant Set Clustering) problem, that is, selecting reference features which form a coherent and most compact set (Section 3.2). Finally, we employ constrained dominant-set-based post-processing step to choose the best matching reference image and use the location of the strongest match as an estimation of the location of the query image (Section 4).

3.1 Dynamic Nearest Neighbor Selection and Query Feature Pruning

For each of N query features detected in the query image, we collect their corresponding nearest neighbors (NN). Let v_m^i be the m th nearest neighbor of i th query feature q^i , and $m \in \mathbb{N} : 1 \leq m \leq |NN^i|$ and $i \in \mathbb{N} : 1 \leq i \leq N$, where $|\cdot|$ represents the set cardinality and NN^i is the set of NNs of the i th query feature. In this work, we propose a dynamic NNs selection technique based on how distinctive two consecutive elements are in a ranked list of neighbors for a given query feature, and employ different number of nearest neighbors for each query feature.

As shown in Algorithm (1), we add the $(m+1)$ th NN of the i th query feature, v_{m+1}^i , if the ratio of the two consecutive NN is greater than θ , otherwise we stop. In other words, in the case of a query feature which is not very discriminative, i.e., most of its NNs are very similar to each other, the algorithm continues adding NNs until a distinctive one is found. In this way, less discriminative query features will use more NNs to account for their ambiguity, whereas more discriminative query features will be compared with fewer NNs.

Algorithm 1. Dynamic Nearest Neighbor Selection for i th Query Feature (q^i)

Input: the i th query feature (q^i) and all its nearest neighbors extracted from K-means tree $\{v_1^i, v_2^i, \dots, v_{|NN^i|}^i\}$

Output: Selected Nearest Neighbors for the i th query feature (\mathbb{V}^i)

```

1: procedure DYNAMIC NN SELECTION
2:   Initialize  $\mathbb{V}^i = \{v_1^i\}$  and  $m=1$ 
3:   while  $m < |NN^i| - 1$  do
4:     if  $\frac{\|\xi(q^i) - \xi(v_m^i)\|}{\|\xi(q^i) - \xi(v_{m+1}^i)\|} > \theta$  then
5:        $\mathbb{V}^i = \mathbb{V}^i \cup v_{m+1}^i$        $\triangleright$  If so, add  $v_{m+1}^i$  to our solution
6:        $m = m + 1$                $\triangleright$  Go to the next neighbor
7:     else
8:       Break                     $\triangleright$  If not, stop adding and exit
9:     end if
10:  end while
11: end procedure

```

Query Feature Pruning. For the geo-localization task, most of the query features that are detected from moving objects (such as cars) or the ground plane, do not convey any useful information. If such features are coarsely identified and removed prior to performing the feature matching, that will reduce the clutter and computation cost for the remaining features. Towards this end, we use the following pruning constraint which takes into consideration distinctiveness of the *first* and the *last* NN. In particular, if $\|\xi(q^i) - \xi(v_1^i)\| / \|\xi(q^i) - \xi(v_{|NN^i|}^i)\| > \beta$, where $\xi(\cdot)$ represents an operator which returns the local descriptor of the argument node, then q^i is removed, otherwise it is retained. That is, if the *first* NN is similar to the *last* NN (less than β), then the corresponding query feature along with its NNs are pruned since it is expected to be uninformative.

We empirically set both thresholds, θ and β , in Algorithm (1) and pruning step, respectively, to 0.7 and keep them fixed for all tests.

3.2 Multiple Feature Matching Using Dominant Sets

3.2.1 The Dominant Set Framework

The dominant set framework is a pairwise clustering approach [37], based on the notion of a dominant set, which can be seen as an edge-weighted generalization of a clique. The approach is a fast and efficient framework for pairwise clustering and has been used to solve multiple problems, such as data association in tracking [38] as well as group detection [39].

In an attempt to formally capture this notion, we present some notations and definitions. The data to be clustered is defined as a graph $G = (V, E, \zeta, \varpi)$, where V, E, ζ and ϖ denote the set of nodes (of cardinality n), edges, node weights and edge weights, respectively. For a non-empty subset $S \subseteq V$, $l \in S$, and $k \notin S$, where l and k represent nodes in a graph G , we define $\phi_S(l, k) = B(l, k) - \frac{1}{|S|} \sum_{p \in S} B(l, p)$, where B is the corresponding $n \times n$ affinity matrix of graph G . This quantity measures the relative similarity between nodes k and l , with respect to the average similarity between node l and its neighbors in S . Note that $\phi_S(l, k)$ can be either positive or negative. Next, to each vertex $i \in S$ we assign a weight defined recursively as follows:

$$W_S(l) = \begin{cases} 1, & \text{if } |S| = 1, \\ \sum_{k \in S \setminus \{l\}} \phi_{S \setminus \{l\}}(k, l) W_{S \setminus \{l\}}(k), & \text{otherwise.} \end{cases} \quad (1)$$

where $S \setminus \{l\}$ means set S without the element l . Intuitively, $W_S(l)$ gives us a measure of the overall similarity between vertex l and the vertices of $S \setminus \{l\}$, with respect to the overall similarity among the vertices in $S \setminus \{l\}$. Therefore, a positive $W_S(l)$ indicates that adding l into its neighbors in S will increase the internal coherence of the set, whereas in the presence of a negative value we expect the overall coherence to be decreased. The total weight of S is computed as $W(S) = \sum_{l \in S} W_S(l)$.

A non-empty subset of vertices $S \subseteq V$ such that $W(T) > 0$ for any non-empty $T \subseteq S$, is said to be a *dominant set* if:

$$\begin{aligned} W_S(l) &> 0, \forall l \in S, \\ W_{S \cup \{l\}}(l) &< 0, \forall l \notin S, \end{aligned} \quad (2)$$

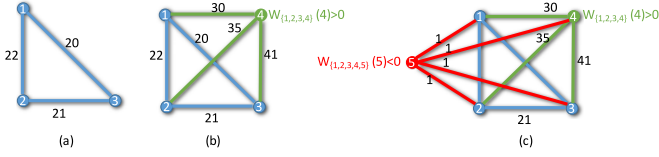


Fig. 2. Dominant set example: (a) shows a compact set (dominant set), (b) node 4 is added which is highly similar to the set $\{1,2,3\}$ forming a new compact set. (c) Node 5 is added to the set which has very low similarity with the rest of the nodes and this is reflected in the value $W_{\{1,2,3,4,5\}}(5)$.

These conditions correspond to the two main properties of a cluster: the first regards internal homogeneity, whereas the second regards external inhomogeneity.

Example. Let us consider a graph with nodes $\{1,2,3\}$, which forms a coherent group (dominant set) with edge weights 20, 21 and 22 as shown in Fig. 2a. Now, let us try to add a node $\{4\}$ to the graph which is highly similar to the set $\{1,2,3\}$ with edge weights of 30, 35 and 41 (see Fig. 2b). Here, we can see that adding node $\{4\}$ to the set increases the overall similarity of the new set $\{1,2,3,4\}$, that can be seen from the fact that the weight associated to the node $\{4\}$ with respect to the set $\{1,2,3,4\}$ is positive, $(W_{\{1,2,3,4\}}(4) > 0)$. On the contrary, when adding node $\{5\}$ which is less similar to the set $\{1,2,3,4\}$ (edge weight of 1 - Fig. 2c) the overall similarity of the new set $\{1,2,3,4,5\}$ decreases, since we are adding to the set something less similar with respect to the internal similarity. This is reflected by the fact that the weight associated to node $\{5\}$ with respect to the set $\{1,2,3,4,5\}$ is less than zero $(W_{\{1,2,3,4,5\}}(5) < 0)$.

From the definition of a dominant set in (2) the set $\{1,2,3,4\}$ (Fig. 2b) forms a dominant set, as it satisfies both criteria (internal coherence and external incoherence). While the weight associated to the node out side of the set (dominant set) is less than zero, $W_{\{1,2,3,4,5\}}(5) < 0$.

The main result presented in [37] provides a one-to-one relation between dominant sets and strict local maximizers of the following standard quadratic optimization problem:

$$\begin{aligned} & \text{maximize} && f(\mathbf{x}) = \mathbf{x}^T \mathbf{B} \mathbf{x}, \\ & \text{subject to} && \mathbf{x} \in \Delta, \end{aligned} \quad (3)$$

where

$$\Delta = \left\{ \mathbf{x} \in \mathbb{R}^n : \sum_i x_i = 1, \text{ and } x_i \geq 0 \text{ for all } i = 1 \dots n \right\},$$

which is called *standard simplex* of \mathbb{R}^n . Specifically, in [37] it is shown that if S is a dominant subset of vertices, then its weighted characteristic vector, which lies in Δ ,

$$x_l = \begin{cases} \frac{W_S(l)}{W(S)}, & \text{if } l \in S, \\ 0, & \text{otherwise} \end{cases}$$

is a strict local solution of (3). Conversely, under mild conditions, if \mathbf{x} is a strict local solution of (3), then its support $S = \sigma(\mathbf{x})$ is a dominant set. Here, the support of a vector $\mathbf{x} \in \Delta$ is the set of indices corresponding to its positive components, that is $\sigma(\mathbf{x}) = \{l \in V : x_l > 0\}$. By virtue of this

result, a dominant set can be found by localizing a local solution of (3) and then picking up its support.

3.2.2 Similarity Function and Dynamics for Multiple Feature Matching

In our framework, the set of nodes, V , represents all NNs for each query feature which survives the pruning step. The edge set is defined as $E = \{(v_m^i, v_n^j) \mid i \neq j\}$, which signifies that all the nodes in G are connected as long as their corresponding query features are not the same. The edge weight, $\varpi : E \rightarrow \mathbb{R}^+$ is defined as $\varpi(v_m^i, v_n^j) = \exp(-\|\psi(v_m^i) - \psi(v_n^j)\|^2 / 2\gamma^2)$, where $\psi(\cdot)$ represents an operator which returns the global descriptor of the parent image of the argument node and γ is empirically set to 2^7 . The global descriptor can be either GPS location (as in this case) or a global image descriptor (such as those described in section 4.1). The edge weight, $\varpi(v_m^i, v_n^j)$, represents a similarity between nodes v_m^i and v_n^j in terms of the global features of their parent images. The node score, $\zeta : V \rightarrow \mathbb{R}^+$, is defined as $\zeta(v_m^i) = \exp(-\|\xi(q^i) - \xi(v_m^i)\|^2 / 2\gamma^2)$. The node score shows how similar the node v_m^i is with its corresponding query feature in terms of its local features.

Matching the query features to the reference features requires identifying the correct NNs from the graph G which maximize the weight, that is, selecting a node (NN) which forms a coherent (highly compact) set in terms of both global and local feature similarities.

Affinity matrix \mathbf{A} represents the global similarity among reference images, which is built using GPS locations as a global feature and a node score \mathbf{b} which shows how similar the reference image is with its corresponding query feature in terms of their local features. We formulate the following optimization problem, a more general form of the dominant set formulation:

$$\begin{aligned} & \text{maximize} && f(\mathbf{x}) = \mathbf{x}^T \mathbf{A} \mathbf{x} + \mathbf{b}^T \mathbf{x}, \\ & \text{subject to} && \mathbf{x} \in \Delta. \end{aligned} \quad (4)$$

The affinity \mathbf{A} and the score \mathbf{b} are computed as follows:

$$\mathbf{A}(v_m^i, v_n^j) = \begin{cases} \varpi(v_m^i, v_n^j), & \text{for } i \neq j, \\ 0, & \text{otherwise,} \end{cases} \quad (5)$$

$$\mathbf{b}(v_m^i) = \zeta(v_m^i). \quad (6)$$

General quadratic optimization problems, like (4), are known to be NP-hard [40]. However, in relaxed form, standard quadratic optimization problems can be solved using many algorithms which make full systematic use of data constellations. Off-the-shelf procedures find a local solution of (4), by following the paths of feasible points provided by game dynamics based on evolutionary game theory.

Interestingly, the general quadratic optimization problem can be rewritten in the form of standard quadratic problem. A principled way to do that is to follow the result presented in [41], which shows that maximizing the general quadratic problem over the simplex can be homogenized as follows. Maximizing $\mathbf{x}^T \mathbf{A} \mathbf{x} + \mathbf{b}^T \mathbf{x}$, subject to $\mathbf{x} \in \Delta$ is equivalent to maximizing $\mathbf{x}^T \mathbf{B} \mathbf{x}$, subject to $\mathbf{x} \in \Delta$, where $\mathbf{B} = \mathbf{A} + \mathbf{e} \mathbf{b}^T + \mathbf{b} \mathbf{e}^T$ and $\mathbf{e} = \sum_{i=1}^n \mathbf{e}_i = [1, 1, \dots, 1]$, where \mathbf{e}_i denotes the

i th standard basis vector in \mathbb{R}^n . This can be easily proved by noting that the problem is solved in the simplex.

$$\begin{aligned} \mathbf{x}^\top \mathbf{A} \mathbf{x} + 2 * \mathbf{b}^\top \mathbf{x} &= \mathbf{x}^\top \mathbf{A} \mathbf{x} + \mathbf{b}^\top \mathbf{x} + \mathbf{x}^\top \mathbf{b}, \\ &= \mathbf{x}^\top \mathbf{A} \mathbf{x} + \mathbf{x}^\top \mathbf{e} \mathbf{b}^\top \mathbf{x} + \mathbf{x}^\top \mathbf{b} \mathbf{e}^\top \mathbf{x}, \\ &= \mathbf{x}^\top (\mathbf{A} + \mathbf{e} \mathbf{b}^\top + \mathbf{b} \mathbf{e}^\top) \mathbf{x}, \\ &= \mathbf{x}^\top \mathbf{B} \mathbf{x}. \end{aligned}$$

As can be inferred from the formulation of our multiple NN feature matching problem, DSC can be essentially used for solving the optimization problem. Therefore, by solving DSC for the graph G , the optimal solution that has the most agreement in terms of local and global features will be found. Next, we introduce some useful dynamics from evolutionary game theory which allow us to efficiently and effectively match reference features to the query features.

The standard approach for finding the local maxima of problem (3), as used in [37], is to use replicator dynamics - a well-known family of algorithms from evolutionary game theory inspired by Darwinian selection processes. Variety of StQP applications [37], [42], [43], [44] have proven the effectiveness of replicator dynamics. However, its computational complexity, which is $O(N^2)$ for problems involving N variables, prevents it from being used in large-scale applications. Its exponential variant, though it reduces the number of iterations needed for the algorithm to find a solution, suffers from a per-step quadratic complexity.

In this work, we adopt a new class of evolutionary game dynamics called infection-immunization dynamics (InIm-Dyn), which have been shown to have a linear time/space complexity for solving standard quadratic programs. In [6], it has been shown that InImDyn is orders of magnitude faster but as accurate as the replicator dynamics.¹

The dynamics, inspired by infection and immunization processes summarized in Algorithm (2), finds the optimal solution by iteratively refining an initial distribution $\mathbf{x} \in \Delta$. The process allows for invasion of an infective distribution $\mathbf{y} \in \Delta$ that satisfies the inequality $(\mathbf{y} - \mathbf{x})^\top \mathbf{B} \mathbf{x} > 0$, and combines linearly \mathbf{x} and \mathbf{y} (line 7 of Algorithm (2)), thereby engendering a new population \mathbf{z} which is immune to \mathbf{y} and guarantees a maximum increase in the expected payoff. A selective function, $\mathcal{S}(\mathbf{x})$, returns an infective strategy for distribution \mathbf{x} if it exists, or \mathbf{x} otherwise (line 2 of Algorithm (2)). Selecting a strategy \mathbf{y} which is infective for the current population \mathbf{x} , the extent of the infection, $\delta_y(\mathbf{x})$, is then computed in lines 3 to 6 of Algorithm (2).

By reiterating this process of infection and immunization the dynamics drives the population to a state that cannot be infected by any other strategy. If this is the case then \mathbf{x} is an equilibrium or fixed point under the dynamics. The refinement loop of Algorithm (2) controls the number of iterations allowing them to continue until \mathbf{x} is within the range of the tolerance τ and we empirically set τ to 10^{-7} . The range $\epsilon(\mathbf{x})$ is computed as $\epsilon(\mathbf{x}) = \sum_{i \in J} \min\{x_i, (\mathbf{B} \mathbf{x})_i - \mathbf{x}^\top \mathbf{B} \mathbf{x}\}^2$.

As it can be inferred from the above formulation of dominant sets, finding the strict local solution of (3) coincides with finding the best matching reference features to the

query features. It is important to note that, since our solution is a local solution and we do not know which local solution includes the best matching reference image, we determine several (typically three) locally optimal solutions. Unlike most of the previous approaches, which perform a simple voting scheme to select the best matching reference image, we introduce a post processing step utilizing a variant of dominant set called *constrained dominant set*, which is discussed briefly in the next section.

Algorithm 2. FindEquilibrium($\mathbf{B}, \mathbf{x}, \tau$)

Input: $n \times n$ payoff matrix \mathbf{B} , initial distribution $\mathbf{x} \in \Delta$ and tolerance τ .

Output: Fixed point \mathbf{x}

1: **while** $\epsilon(\mathbf{x}) > \tau$ **do**

2: $\mathbf{y} \leftarrow \mathcal{S}(\mathbf{x})$

3: $\delta \leftarrow 1$

4: **if** $(\mathbf{y} - \mathbf{x})^\top \mathbf{B}(\mathbf{y} - \mathbf{x}) < 0$ **then**

5: $\delta \leftarrow \min\left\{\frac{(\mathbf{x} - \mathbf{y})^\top \mathbf{B} \mathbf{x}}{(\mathbf{y} - \mathbf{x})^\top \mathbf{B}(\mathbf{y} - \mathbf{x})}, 1\right\}$

6: **end if**

7: $\mathbf{x} \leftarrow \delta(\mathbf{y} - \mathbf{x}) + \mathbf{x}$

8: **end while**

9: **return** \mathbf{x}

4 POST PROCESSING USING CONSTRAINED DOMINANT SETS

Up to now, we devised a method to collect matching reference features corresponding to our query features. The next task is to select one reference image, based on feature matching between query and reference features, which best matches the query image.

To do so, most of the previous methods follow a simple voting scheme, where the matched reference image with the highest vote is considered as the best match. This approach has two important shortcomings. First, if there are equal votes for two or more reference images (which happens quite often), it will randomly select one, which makes it prone to outliers. Second, a simple voting scheme does not consider the similarity between the query image and the candidate reference images at the global level, but simply accounts for local matching of features. Therefore, we deal with this issue by proposing a post processing step, which considers the comparison of the global features of the images and employs *constrained dominant set*, a framework that generalizes the dominant sets formulation [37], [45].

4.1 Constrained Dominant Sets Framework

In our post processing step, the user-selected query and the matched reference images are related using their *global* features and a unique local solution is then searched which contains the union of all the dominant sets containing the query. As customary, the resulting solution will be globally consistent both with the reference images and the query image and due to the notion of *centrality*, each element in the resulting solution will have a membership score, which depicts how similar a given reference image is with the rest of the images in the cluster. So, by virtue of this property of constrained dominant sets, we will select the image with the highest membership score as the final best matching

1. A practical implementation is available at <https://github.com/xwasco/DominantSetLibrary>

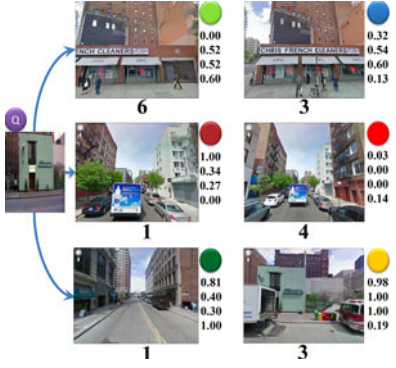


Fig. 3. Exemplar output of the dominant set framework: *Left*: query, *Right*: each row shows corresponding reference images from the first, second and third local solutions (dominant sets), respectively, from top to bottom. The number under each image shows the frequency of the matched reference image, while those on the right side of each image show the min-max normalized scores of HSV, CNN6, CNN7 and GIST global features, respectively. The filled colors circles on the upper right corner of the images are used as reference IDs of the images.

reference image and approximate the location of the query with the GPS location of the best matched reference image.

In this section, we review the basic definitions and properties of constrained dominant sets, as introduced in [46]. Given a user specified query, $Q \subseteq \hat{V}$, we define the graph $\hat{G} = (\hat{V}, \hat{E}, \hat{w})$, where the edges are defined as $\hat{E} = \{(i, j) | i \neq j, \{i, j\} \in \mathcal{DS}_n \vee (i \in Q \vee j \in Q)\}$, i.e., all the nodes are connected as long as they do not belong to different local maximizers, \mathcal{DS}_n , which represents the n th extracted dominant set. The set of nodes \hat{V} represents all matched reference images (local maximizers) and query image, Q . The edge weight $\hat{w} : \hat{E} \rightarrow \mathbb{R}^+$ is defined as,

$$\hat{w}(i, j) = \begin{cases} \rho(i, j), & \text{for } i \neq j, (i \in Q \wedge j \in \mathcal{DS}_n) \vee (i \in \mathcal{DS}_n \wedge j \in Q), \\ B_n(i, j), & \text{for } i \neq j, \{i, j\} \in \mathcal{DS}_n, \\ 0, & \text{otherwise} \end{cases}$$

where $\rho(i, j)$ is an operator which returns the global similarity of two given images i and j , that is, $\rho(i, j) = \exp(-\|\psi(i) - \psi(j)\|^2 / 2\gamma^2)$, B_n represents a sub-matrix of B , which contains only members of \mathcal{DS}_n , normalized by its maximum value and finally $B_n(i, j)$ returns the normalized affinity between the i th and j th members of \mathcal{DS}_n . The graph \hat{G} can be represented by an $n \times n$ affinity matrix $\hat{B} = (\hat{w}(i, j))$, where n is the number of nodes in the graph.

Given a parameter $\alpha > 0$, let us define the following parameterized variant of program (3):

$$\begin{aligned} & \text{maximize} && f_Q^\alpha(\mathbf{x}) = \mathbf{x}^\top (\hat{B} - \alpha \hat{I}_Q) \mathbf{x}, \\ & \text{subject to} && \mathbf{x} \in \Delta, \end{aligned} \quad (7)$$

where \hat{I}_Q is the $n \times n$ diagonal matrix whose diagonal elements are set to 1 in correspondence to the vertices contained in $\hat{V} \setminus Q$ (a set \hat{V} without the element Q) and to zero otherwise.

Let $Q \subseteq \hat{V}$, with $Q \neq \emptyset$ and let $\alpha > \lambda_{\max}(\hat{B}_{\hat{V} \setminus Q})$, where $\lambda_{\max}(\hat{B}_{\hat{V} \setminus Q})$ is the largest eigenvalue of the principal sub-matrix of \hat{B} indexed by the elements of $\hat{V} \setminus Q$. If \mathbf{x} is a local maximizer of f_Q^α in Δ , then $\sigma(\mathbf{x}) \cap Q \neq \emptyset$. A complete proof can be found in [46].

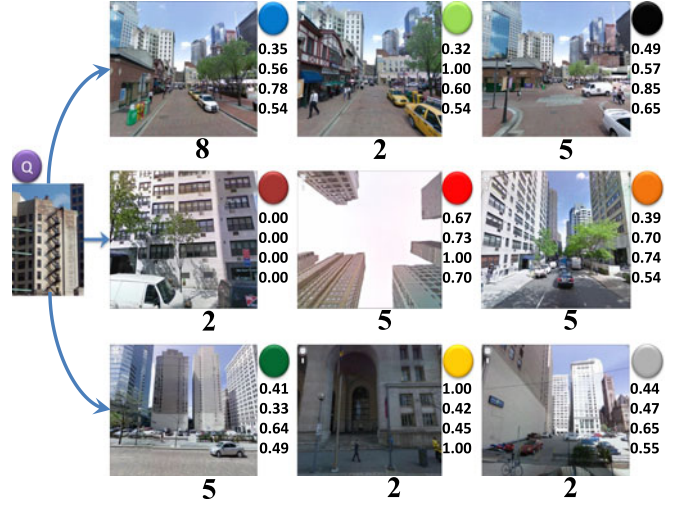


Fig. 4. Another exemplar output of the dominant set framework. See caption of Fig. 3 for details.

The above result provides us with a simple technique to determine dominant-set clusters containing user-specified query vertices: if Q is a vertex selected by the user, by setting

$$\alpha > \lambda_{\max}(\hat{B}_{\hat{V} \setminus Q}), \quad (8)$$

we are guaranteed that all local solutions of (7) will have a support that necessarily contains elements of Q .

The similarity between query Q and the corresponding matched reference images is computed using their global features such as HSV histogram, GIST [47] and CNN.² For the different advantages and disadvantages of the global features, we refer interested readers to [2].

The performance of our post processing may vary dramatically among queries and we do not know in advance which global feature plays a major role. Figs. 3 and 4 show illustrative cases of different global features. In the case of Fig. 3, HSV color histograms and GIST provide a wrong match (dark red node for HSV and dark green node for GIST), while both CNN-based global features (CNN6 and CNN7) matched it to the right reference image (yellow node). The second example, Fig. 4, shows us that only CNN6 feature localized it to the right location while the others fail. Recently, fusing different retrieval methods has been shown to enhance the overall retrieval performance [49], [50].

Motivated by [49] we dynamically assign a weight, based on the effectiveness of a feature, to all global features based on the area under normalized score between the query and the matched reference images. The area under the curve is inversely proportional to the effectiveness of a feature. More specifically, let us suppose to have \mathcal{G} global features and the distance between the query and the j th matched reference image (\mathcal{N}_j), based on the i th global feature (\mathcal{G}_i), is computed as: $f_i^j = \psi_i(Q) - \psi_i(\mathcal{N}_j)$, where $\psi_i(\cdot)$ represents an operator which returns the i th global image descriptor of the argument node. Let the area under the normalized score

2. CNN6 and CNN7 are Convolutional Neural Network features extracted from ReLU6 and FC7 layers of pre-trained network, respectively [48].

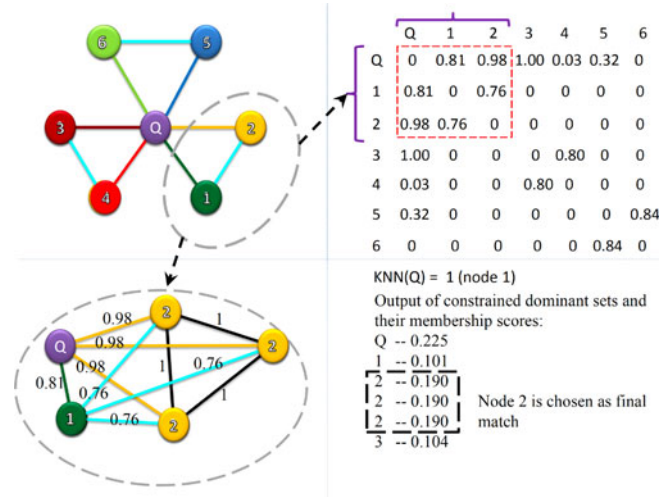


Fig. 5. Exemplar graph for post processing. *Top left:* reduced graph for Fig. 3 which contains unique matched reference images. *Bottom left:* Part of the full graph which contains the gray circled nodes of the reduced graph and the query. Since the frequency of images represented by a yellow node in Fig. 3 is 3, we represent it with 3 nodes in the expanded graph. The same is true for all nodes. *Top right:* corresponding affinity of the reduced graph. *Bottom right:* The outputs of nearest neighbor approach, consider only the node's pairwise similarity, ($KNN(Q) = \text{node 3}$ which is the dark red node) and constrained dominant sets approach ($CDS(Q) = \text{node 2}$ which is the yellow node).

of f_i be \mathcal{A}_i . The weight assigned for feature \mathcal{G}_i is then computed as $w_i = \frac{1}{\mathcal{A}_i} / \sum_{j=1}^{|\mathcal{G}|} \frac{1}{\mathcal{A}_j}$.

Figs. 3 and 4 show illustrative cases of some of the advantages of having the post processing step. Both cases show the disadvantage of localization following heuristic approaches, as in [1], [2], to voting and selecting the reference image that matches to the query. In each case, the matched reference image with the highest number of votes (shown under each image) is the first node of the first extracted dominant set, but represents a wrong match. Both cases (Figs. 3 and 4) also demonstrate that the KNN-based matching may lead to a wrong localization. For example, by choosing HSV histogram as a global feature, the KNN approach chooses as best match the dark red node in Fig. 3 and the yellow node in Fig. 4 (both with min-max value to 1.00). Moreover, it is also evident that choosing the best match using the first extracted local solution (i.e., the light green node in Fig. 3 and blue node in Fig. 4), as done in [2], may lead to a wrong localization, since one cannot know in advance which local solution plays a major role. In fact, in the case of Fig. 3, the third extracted dominant set contains the right matched reference image (yellow node), whereas in the case of Fig. 4 the best match is contained in the first local solution (the light green node).

Fig. 3 shows the top three extracted dominant sets with their corresponding frequency of the matched reference images (at the bottom of each image). Let \mathcal{F}_i be the number (cardinality) of local features, which belongs to i th reference image from the extracted sets and the total number of matched reference images be \mathcal{N} . We build an affinity matrix \hat{B} of size $\mathcal{S} = \sum_{i=1}^{\mathcal{N}} \mathcal{F}_i + 1$ (e.g., for the example in Fig. 3, the size \mathcal{S} is 19). Fig. 5 shows the reduced graph for the matched reference images shown in Fig. 3. Fig. 5 upper left, shows the part of the graph for the post processing. It shows

the relation that the query has with matched reference images. The bottom left part of the figure shows how one can get the full graph from the reduced graph. For the example in Fig. 5, $\hat{V} = \{Q, 1, 2, 2, 2, 3, 4, 4, \dots, 6\}$.

The advantages of using constrained dominant sets are numerous. First, it provides a unique local (and hence global) solution whose support coincides with the union of all dominant sets of \hat{G} , which contains the query. Such solution contains all the local solutions which have strong relation with the user-selected query. As it can be observed in Fig. 5 (bottom right), the Constrained Dominant Set which contains the query Q , $CDS(Q)$, is the union of all overlapping dominant sets (the query, one green, one dark red and three yellow nodes) containing the query as one of the members. If we assume to have no cyan link between the green and yellow nodes, as long as there is a strong relation between the green node and the query, $CDS(Q)$ will not be affected. In addition, due to the noise, the strong affinity between the query and the green node may be reduced, while still keeping the strong relation with the cyan link which, as a result, will preserve the final result. Second, in addition to fusing all the local solutions leveraging the notion of centrality, one of the interesting properties of dominant set framework is that it assigns to each image a score corresponding to how similar it is to the rest of the images in the solution. Therefore, not only it helps selecting the best local solution, but also choosing the best final match from the chosen local solution. Third, an interesting property of constrained dominant sets approach is that it not only considers the pairwise similarity of the query and the reference images, but also the similarity among the reference images. This property helps the algorithm avoid assignment of wrong high pairwise affinities. As an example, with reference to Fig. 5, if we consider the nodes pairwise affinities, the best solution will be the dark red node (score 1.00). However, using constrained dominant sets and considering the relation among the neighbors, the solution bounded by the red dotted rectangle can be found, and by choosing the node with the highest membership score, the final best match is the yellow node which is more similar to the query image than the reference image in the dark red node.

5 EXPERIMENTAL RESULTS

5.1 Dataset Description

We evaluate the proposed algorithm using publicly available reference data sets of over 102k Google street view images [2] and a new dataset, *WorldCities*, of high resolution 300k Google street view images collected for this work. The 360 degrees view of each place mark is broken down into one top and four side view images. The *WorldCities* dataset is publicly available.³

The 102k Google street view images dataset covers 204 Km of urban streets and the place marks are approximately 12 m apart. It covers downtown and the neighboring areas of Orlando, FL; Pittsburgh, PA and partially Manhattan, NY. The *WorldCities* dataset is a new high resolution reference dataset of 300k street view images that covers 14 different cities from different parts of the world: Europe

3. <http://www.cs.ucf.edu/~haroon/UCF-Google-Streetview-II-Data/UCF-Google-Streetview-II-Data.zip>



Fig. 6. The top four rows are sample street view images from eight different places of **WorldCities** dataset. The bottom two rows are sample user uploaded images from the test set.

(Amsterdam, Frankfurt, Rome, Milan and Paris), Australia (Sydney and Melbourne), USA (Vegas, Los Angeles, Phoenix, Houston, San Diego, Dallas, Chicago). Existence of similarity in buildings around the world, which can be in terms of their wall designs, edges, shapes, color etc, makes the dataset more challenging than the other. Fig. 6 (top four rows) shows sample reference images taken from different place marks.

For the test set, we use 644 and 500 GPS-tagged user uploaded images downloaded from Picasa, Flickr and Panoramio for the 102k Google street view images and **WorldCities** datasets, respectively. Fig. 6 (last two rows) shows sample test images. Throughout our experiment, we use all the reference images from around the world to find the best match with the query image, not just with the ground truth city only.

5.2 Quantitative Comparison with Other Methods

5.2.1 Performance on the 102k Google Street View Dataset

The proposed approach has been then compared with the results obtained by state-of-the-art methods. In Fig. 7, the horizontal axes shows the error threshold in meters, while the vertical one shows the percentage of the test set localized within a specific error threshold. Since the scope of this work is an accurate image localization at a city-scale level, test images localized above 300 meters are considered a failure.

The black (-*-) curve shows localization result of the approach proposed in [4] which uses vocabulary tree to localize images. The red (-o-) curve depicts the results of [1] where they only consider the first NN for each query feature as best matches which makes the approach very sensitive to the query features they select. Moreover, their approach suffers from lacking global feature information. The green (-o-) curve illustrates the localization results of [2] which uses generalized maximum clique problem (GMCP) to solve feature matching problem and follows voting scheme to select the best matching reference image. The

black (-o- and -◇-) curves show localization results of MAC and RMAC, (regional) maximum activation of convolutions ([51], [52]). These approaches build compact feature vectors that encode several image regions without the need to feed multiple inputs to the network. The cyan (-o-) curve represents localization result of NetVLAD [16] which aggregates mid-level (conv5) convolutional features extracted from the entire image into a compact single vector representation amenable to efficient indexing. The cyan (-◇-) curve depicts localization result of NetVLAD but finetuned on our dataset. The blue (-◇-) curve show localization result of approach proposed in [15] which exploits geometric relations between different database images retrieved by a query to handle geometric burstness. The blue (-o-) curve shows results from our baseline approach, that is, we use voting scheme to select best match reference image and estimate the location of the query image. We

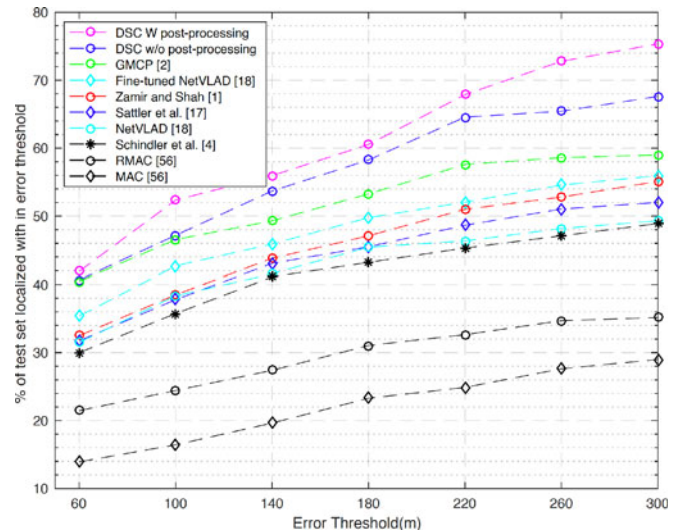


Fig. 7. Comparison of our baseline (without post processing) and final method with state-of-the-art approaches on the first dataset (102K Google street view images).

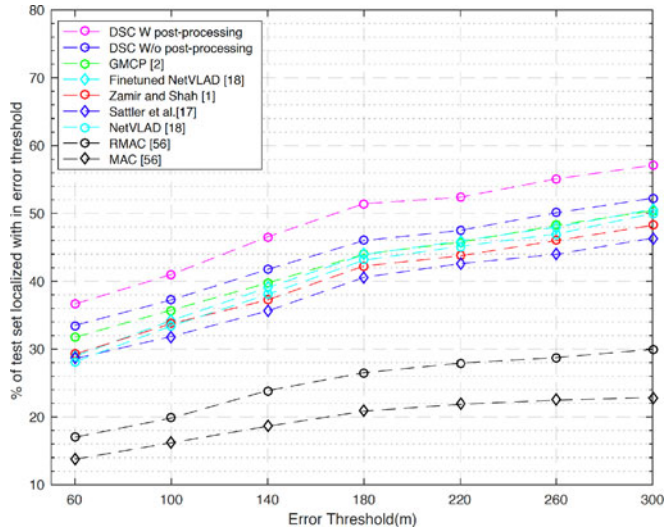


Fig. 8. Comparison of overall geo-localization results using DSC with and without post processing and state-of-the-art approaches on the *WorldCities* dataset.

are able to make a 10 percent improvement w.r.t the other methods with only our baseline approach (without post processing). The magenta (—○—) curve illustrates geo-localization results of our proposed approach using dominant set clustering based feature matching and constrained dominant set clustering based post processing.

Fig. 7 shows the results of the comparison. As it can be seen, our baseline approach can significantly outperform existing methods by simply employing a voting scheme as a post processing. Moreover, we further boost our results by using constrained dominant sets as a post-processing step.

The proposed approach has several advantages over the above-mentioned approaches, as most approaches depend only on a pairwise affinity between query and

reference images to select the best matching reference image, they are prone to outliers. For instance, some reference images appear similar to the query while they are from a different geographical location. However, in our case, first, during candidate reference image matching step employing dominant set clustering, location of reference image is used as a cost in addition to the visual features to ensure both visual similarity and geographical proximity of elements within candidate dominant sets. Second, in the proposed post processing step, the final selected reference image should not be only similar to the query but also needs to be consistent with members of the extracted cluster (constrained dominant set), which are also similar to the query.

As it can be seen, our approach shows about 20 percent improvement over the state-of-the-art techniques.

5.2.2 Performance on the WorldCities Dataset

We have also compared the performance of different algorithms on the new dataset of 300k Google street view images created by us. Similarly to the previous tests, Fig. 8 reports the percentage of the test set localized within a particular error threshold. Since the new dataset is relatively more challenging, the overall performance achieved by all the methods is lower compared to 102k image dataset.

From bottom to top of the graph in Fig. 8 we present the results of [51], [52] black (—◇— and —○—), [15] blue (—◇—), [1] red (—○—), [16] cyan (—○—), fine tuned [16] cyan (—◇—), [2] green (—○—), our baseline approach without post processing blue (—○—) and our final approach with post processing magenta (—○—). The improvements obtained with our method are lower than in the other dataset, but still noticeable (around 2 percent for the baseline and 7 percent for the final approach). Some qualitative results for Pittsburgh, PA are presented in Fig. 9.

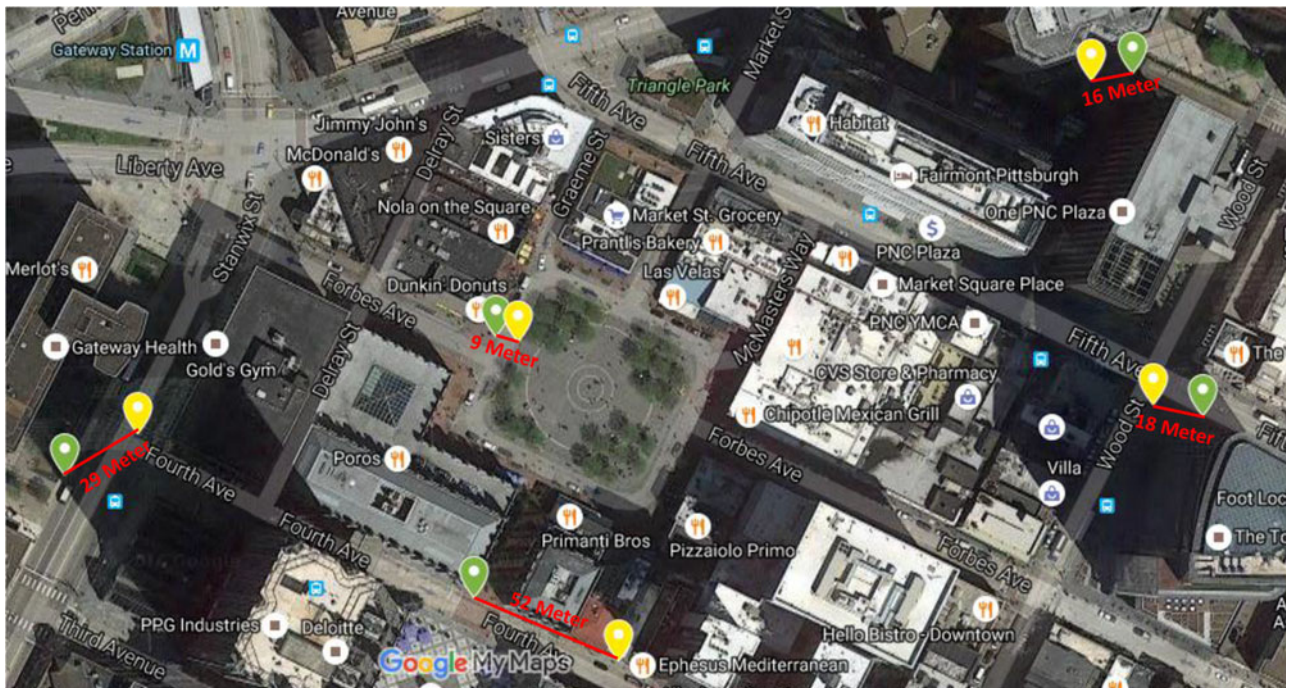


Fig. 9. Sample qualitative results taken from Pittsburgh area. The green ones are the ground truth while yellow locations indicate our localization results.

TABLE 1
Performance on San Francisco Dataset

Method	recall first rank
Chen et al. [53]	41%
Zhang et al. [50]	62%
Torii et al. [17]	63%
Arandjelović and Zisserman [31]	72%
Tolias et al. [54]	76%
Our method	62%

5.2.3 Performance on San Francisco Dataset

Although the focus of the proposed approach is to solve coarse-level image localization, we also tested our method on the San Francisco dataset of Chen et al. [53]. This dataset contains densely-collected images from only one city to test the performance of algorithms in estimating the location at a city scale. The results reported in Table 1 use 1.06 M perspective central images (PCI) extracted from panoramas as the database photos, and the original 803 test images as queries. Both the database images and the queries come with building IDs, which are used to test the performance. The results summarized in Table 1 consider a localization as correct if the query image is localized to point at the correct building ID according to the ground truth annotation. We report the recall on the first ranked images, i.e., the recall of each query to find the correct result as first in the ranking. This measure is averaged over all queries. Note that the main objective of our proposed method is coarse level localization covering many cities of the world, not densely collected dataset like San Francisco. Some more specific adjustments to our method should be made to reach state-of-the-art results on this dataset, which is out of scope of this paper.

5.3 Analysis

5.3.1 Outlier Handling

In order to show that our dominant set-based feature matching technique is robust in handling outliers, we conduct an experiment by fixing the number of NNs (disabling the dynamic selection of NNs) to different numbers. It is obvious that the higher the number of NNs are considered for each query feature, the higher will be the number of outlier NNs in the input graph, besides the increased computational cost

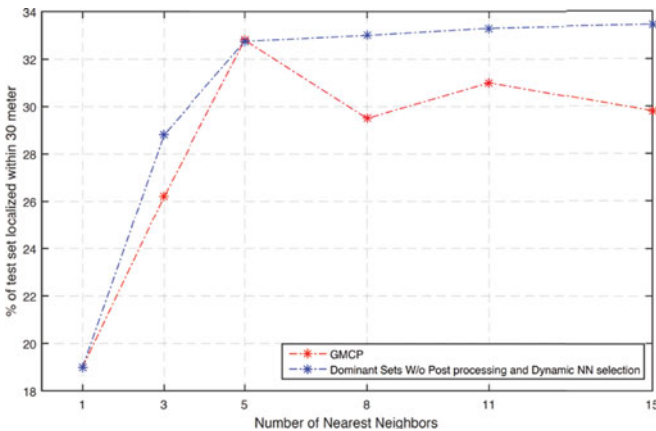


Fig. 10. Results with different number of NN.

TABLE 2
Results of the Experiment, Done on the 102k Google Street View Images (Dts1) and **WorldCities** (Dts2) Datasets, to See the Impact of the Post-Processing Step When the Candidates of Reference Images Are Obtained by Other Image Retrieval Algorithms

		NetVLAD	NetVLAD*	RMAC	MAC
Dts 1	Rank1	49.20	56.00	35.16	29.00
	w_post	51.60	58.05	40.18	36.30
Dts 2	Rank1	50.00	50.61	29.96	22.87
	w_post	53.04	52.23	33.16	26.31

and an elevated chance of query features whose NNs do not contain any inliers surviving the pruning stage.

Fig. 10 shows the results of geo-localization obtained by using GMCP and dominant set based feature matching on 102 K Google street view images [2]. The graph shows the percentage of the test set localized within the distance of 30 meters as a function of number of NNs. The blue curve shows the results using dominant sets: it is evident that when the number of NNs increases, the performance improves despite the fact that more outliers are introduced in the input graph. This is mainly because our framework takes advantage of the few inliers that are added along with many outliers. The red curve shows the results of GMCP based localization and as the number of NNs increase the results begin to drop. This is mainly due to the fact that their approach imposes hard constraint that at least one matching reference feature should be selected for each query feature whether or not the matching feature is correct.

5.3.2 Effectiveness of the Proposed Post Processing

In order to show the effectiveness of the post processing step, we perform an experiment comparing our constrained dominant set based post processing with our baseline (a simple voting scheme) to select the best matching reference image. In Figs. 7 and 8, blue (—o—) and magenta (—o—) curves depict our geo-localization results, without and with post processing, respectively. It is evident from the results, in both experiments, that using constrained dominant sets as a post-processing step significantly boosts the results, as compared to employing a simple voting scheme (baseline) to select the final best matching reference image.

As our post-processing algorithm can be easily plugged in to an existing retrieval methods, we perform another experiment to determine how much improvement we can achieve by our post processing. We use [16], [51], [52] methods to obtain candidate reference images and employ as an edge weight the similarity score generated by the corresponding approaches. Table 2 reports, for each dataset, the first row shows rank-1 result obtained from the existing algorithms while the second row (w_post) shows rank-1 result obtained after adding the proposed post-processing step on top of the retrieved images and 300m is used as a distance threshold for evaluation. For each query, we use the first 20 retrieved reference images. As the results demonstrate, Table 2, we are able to make up to 7 and 4 percent improvement on 102k Google street view images and *WorldCities* datasets, respectively. We ought to note that, the total additional time required to perform the above post

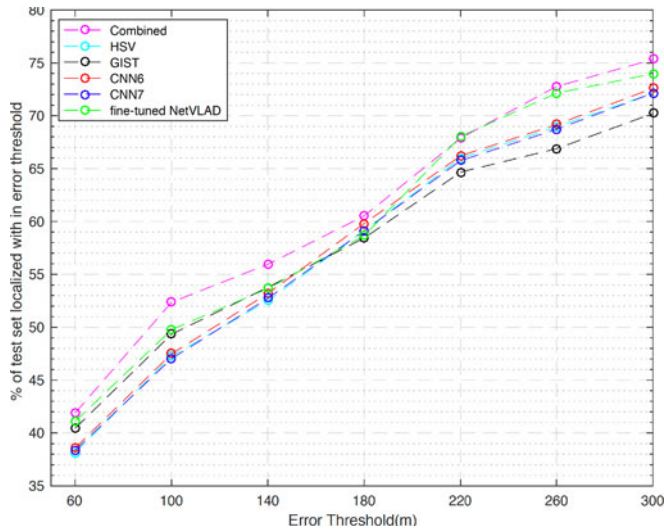


Fig. 11. Comparison of geo-localization results using different global features for our post processing step.

processing, for each approach, is less than 0.003 seconds on average.

The NetVLAD results are obtained from the features generated using the best trained model downloaded from the authors project page [16]. It's fine-tuned version (NetVLAD*) is obtained from the model we fine-tuned using images within 24 m range as a positive set and images with GPS locations greater than 300 m as a negative set.

The MAC and RMAC results are obtained using MAC and RMAC representations extracted from fine-tuned VGG networks downloaded from the authors webpage [51], [52].

5.3.3 Assessment of Global Features Used in Post Processing Step

The input graph for our post processing step utilizes the global similarity between the query and the matched reference images. Wide variety of global features can be used for the proposed technique. In our experiments, the similarity between query and the corresponding matched reference images is computed between their global features, using HSV, GIST, CNN6, CNN7 and fine-tuned NetVLAD. The performance of the proposed post processing technique highly depends on the discriminative ability of the global features used to build the input graph.

Depending on how informative the feature is, we dynamically assign a weight for each global feature based on the area under the normalized score between the query and the matched reference images. To show the effectiveness of this approach, we perform an experiment to find the location of our test set images using both individual and combined global features. Fig. 11 shows the results attained by using fine-tuned NetVLAD, CNN7, CNN6, GIST, HSV and by combining them together. The combination of all the global features outperforms the individual feature performance, demonstrating the benefits of fusing the global features based on their discriminative abilities for each query.

Space and Computational Time. Most retrieval systems are characterized by a large memory requirement. For instance, among the most recent, NetVLAD [17] requires 4096 (feature dimension) \times 4 bytes (single precision) and RMAC [52] requires 512 (feature dimension) \times 4 bytes. Moreover, most of

the methods perform a very costly runtime spatial verification (SV), which requires storing thousands of local descriptors for each image in the database. Several approaches have been proposed in attempt to determine the trade-off between reducing memory footprint (storage) and retrieval efficiency. Compressing image descriptors using principal component analysis (PCA) and different quantization techniques led to research themes on the trade-off between memory footprint of an image descriptor and retrieval performance. Our approach, in the current form, has the same limitations. However, partitioning the space or parallelizing on distributed machines is a possible solution, and replacing tree-based approximate nearest neighbor to product quantization [55] can solve these limitations.

Regarding the computational time (running on a machine with 164 GB RAM, core i7 of 3.1 GHz), the methods like NetVLAD and RMAC [17], [52], take fraction of seconds to rank and localize the query (after feature extraction). In our framework, the main limitation regarding the computational time is the nearest neighbor search, which can be replaced by many different searching algorithms. In the tree search algorithm that we use, the nearest neighbor search, from a tree built using more than 40 million SIFT features of the first dataset (102 K Google street view images), took around 3 secs. The SIFT feature extraction, DSC and the post processing steps are very fast (fractions of seconds).

6 CONCLUSION AND FUTURE WORK

In this paper, we proposed a novel framework for city-scale image geo-localization. Specifically, we introduced dominant set clustering-based multiple NN feature matching approach. Both global and local features are used in our matching step in order to improve the matching accuracy. In the experiments, carried out on two large city-scale datasets, we demonstrated the effectiveness of post processing employing the novel constrained dominant set over a simple voting scheme. Furthermore, we showed that our proposed approach is 200 times, on average, faster than GMCP-based approach [2]. Finally, the newly-created dataset (*WorldCities*) containing more than 300k Google Street View images used in our experiments is available to the public for research purposes.

As a natural future direction of research, we can extend the results of this work for estimating the geo-spatial trajectory of a video in a city-scale urban environment from a moving camera with unknown intrinsic camera parameters.

ACKNOWLEDGMENTS

Eyasu Zemene and Yonatan Tariku Tesfaye are contributed equally to this work.

REFERENCES

- [1] A. R. Zamir and M. Shah, "Accurate image localization based on google maps street view," in *Proc. Eur. Conf. Comput. Vis.*, 2010, pp. 255–268.
- [2] A. R. Zamir and M. Shah, "Image Geo-localization based on multiple nearest neighbor feature matching using generalized graphs," *IEEE Trans. Pattern Anal. Mach. Intell.*, vol. 36, no. 8, pp. 1546–1558, Aug. 2014.
- [3] J. Hays and A. A. Efros, "Im2gps: estimating geographic information from a single image," in *Proc. IEEE Conf. Comput. Vis. Pattern Recognit.*, 2008, pp. 1–8.

- [4] G. Schindler, M. A. Brown, and R. Szeliski, "City-scale location recognition," in *Proc. IEEE Comput. Soc. Conf. Comput. Vis. Pattern Recognit.*, 2007, pp. 1–7.
- [5] S. RotaBulò and I. M. Bomze, "Infection and immunization: A new class of evolutionary game dynamics," *Games Econom. Behavior*, vol. 71, no. 1, pp. 193–211, 2011.
- [6] S. R. Bulò, M. Pelillo, and I. M. Bomze, "Graph-based quadratic optimization: A fast evolutionary approach," *Comput. Vis. Image Understanding*, vol. 115, no. 7, pp. 984–995, 2011.
- [7] Y. Avrithis, Y. Kalantidis, G. Toliás, and E. Spyrou, "Retrieving landmark and non-landmark images from community photo collections," in *Proc. 18th ACM Int. Conf. Multimedia*, 2010, pp. 153–162.
- [8] D. M. Chen, et al., "City-scale landmark identification on mobile devices," in *Proc. IEEE Conf. Comput. Vis. Pattern Recognit.*, 2011, pp. 737–744.
- [9] T. Quack, B. Leibe, and L. Van Gool, "World-scale mining of objects and events from community photo collections," in *Proc. Int. Conf. Content-Based Image Video Retrieval*, 2008, pp. 47–56.
- [10] Y.-T. Zheng, et al., "Tour the world: building a web-scale landmark recognition engine," in *Proc. IEEE Conf. Comput. Vis. Pattern Recognit.*, 2009, pp. 1085–1092.
- [11] H. Jin Kim, E. Dunn, and J.-M. Frahm, "Predicting good features for image geo-localization using per-bundle vlad," in *Proc. IEEE Int. Conf. Comput. Vis.*, 2015, pp. 1170–1178.
- [12] J. Hays and A. A. Efros, "Large-scale image geolocalization," in *Multimodal Location Estimation of Videos and Images*. Berlin, Germany: Springer, 2015, pp. 41–62.
- [13] T. Weyand, I. Kostrikov, and J. Philbin, "Planet-photo geolocation with convolutional neural networks," *ECCV*, pp. 37–55, 2016.
- [14] D. J. Crandall, L. Backstrom, D. Huttenlocher, and J. Kleinberg, "Mapping the world's photos," in *Proc. 18th Int. Conf. World Wide Web*, 2009, pp. 761–770.
- [15] T. Sattler, M. Havlena, K. Schindler, and M. Pollefeys, "Large-scale location recognition and the geometric burstiness problem," in *Proc. IEEE Conf. Comput. Vis. Pattern Recognit.*, 2016, pp. 1582–1590.
- [16] R. Arandjelovic, P. Gronat, A. Torii, T. Pajdla, and J. Sivic, "Netvlad: CNN architecture for weakly supervised place recognition," in *Proc. IEEE Conf. Comput. Vis. Pattern Recognit.*, 2016, pp. 5297–5307.
- [17] A. Torii, J. Sivic, M. Okutomi, and T. Pajdla, "Visual place recognition with repetitive structures," *IEEE Trans. Pattern Anal. Mach. Intell.*, vol. 37, no. 11, pp. 2346–2359, Nov. 2015.
- [18] B. Zeisl, T. Sattler, and M. Pollefeys, "Camera pose voting for large-scale image-based localization," in *Proc. IEEE Int. Conf. Comput. Vis.*, 2015, pp. 2704–2712.
- [19] S. Agarwal, N. Snavely, I. Simon, S. M. Seitz, and R. Szeliski, "Building rome in a day," in *Proc. IEEE 12th Int. Conf. Comput. Vis.*, 2009, pp. 72–79.
- [20] Y. Li, N. Snavely, D. Huttenlocher, and P. Fua, "Worldwide pose estimation using 3d point clouds," in *Proc. Eur. Conf. Comput. Vis.*, 2012, pp. 15–29.
- [21] T. Sattler, B. Leibe, and L. Kobbelt, "Improving image-based localization by active correspondence search," in *Proc. Eur. Conf. Comput. Vis.*, 2012, pp. 752–765.
- [22] E. Kalogerakis, O. Vesselova, J. Hays, A. A. Efros, and A. Hertzmann, "Image sequence geolocation with human travel priors," in *Proc. IEEE 12th Int. Conf. Comput. Vis.*, 2009, pp. 253–260.
- [23] G. Vaca-Castano, A. R. Zamir, and M. Shah, "City scale geospatial trajectory estimation of a moving camera," in *Proc. IEEE Conf. Comput. Vis. Pattern Recognit.*, 2012, pp. 1186–1193.
- [24] A. Hakeem, R. Vezzani, M. Shah, and R. Cucchiara, "Estimating geospatial trajectory of a moving camera," in *Proc. 18th Int. Conf. Pattern Recognit.*, 2006, pp. 82–87.
- [25] C.-Y. Chen and K. Grauman, "Clues from the beaten path: Location estimation with bursty sequences of tourist photos," in *Proc. IEEE Conf. Comput. Vis. Pattern Recognit.*, 2011, pp. 1569–1576.
- [26] T.-Y. Lin, S. Belongie, and J. Hays, "Cross-view image geolocalization," in *Proc. IEEE Conf. Comput. Vis. Pattern Recognit.*, 2013, pp. 891–898.
- [27] T.-Y. Lin, Y. Cui, S. Belongie, and J. Hays, "Learning deep representations for ground-to-aerial geolocalization," in *Proc. IEEE Conf. Comput. Vis. Pattern Recognit.*, 2015, pp. 5007–5015.
- [28] S. Workman, R. Souvenir, and N. Jacobs, "Wide-area image geolocalization with aerial reference imagery," in *Proc. IEEE Int. Conf. Comput. Vis.*, 2015, pp. 3961–3969.
- [29] N. Jacobs, S. Satkin, N. Roman, R. Speyer, and R. Pless, "Geolocating static cameras," in *Proc. IEEE 11th Int. Conf. Comput. Vis.*, 2007, pp. 1–6.
- [30] S. Ramalingam, S. Bouaziz, P. Sturm, and M. Brand, "Skyline2gps: Localization in urban canyons using omni-skylines," in *Proc. IEEE/RSJ Int. Conf. Intell. Robots Syst.*, 2010, pp. 3816–3823.
- [31] R. Arandjelović and A. Zisserman, "Dislocation: Scalable descriptor distinctiveness for location recognition," in *Proc. Asian Conf. Comput. Vis.*, 2014, pp. 188–204.
- [32] A. Bergamo, S. N. Sinha, and L. Torresani, "Leveraging structure from motion to learn discriminative codebooks for scalable landmark classification," in *Proc. IEEE Conf. Comput. Vis. Pattern Recognit.*, 2013, pp. 763–770.
- [33] S. Cao and N. Snavely, "Graph-based discriminative learning for location recognition," in *Proc. IEEE Conf. Comput. Vis. Pattern Recognit.*, 2013, pp. 700–707.
- [34] P. Gronat, G. Obozinski, J. Sivic, and T. Pajdla, "Learning and calibrating per-location classifiers for visual place recognition," in *Proc. IEEE Conf. Comput. Vis. Pattern Recognit.*, 2013, pp. 907–914.
- [35] Q. Hao, R. Cai, Z. Li, L. Zhang, Y. Pang, and F. Wu, "3d visual phrases for landmark recognition," in *Proc. IEEE Conf. Comput. Vis. Pattern Recognit.*, 2012, pp. 3594–3601.
- [36] M. Muja and D. G. Lowe, "Fast approximate nearest neighbors with automatic algorithm configuration," in *Proc. 4th Int. Conf. Comput. Vis. Theory Appl.*, 2009, pp. 331–340.
- [37] M. Pavan and M. Pelillo, "Dominant sets and pairwise clustering," *IEEE Trans. Pattern Anal. Mach. Intell.*, vol. 29, no. 1, pp. 167–172, Jan. 2007.
- [38] Y. T. Tesfaye, E. Zemene, M. Pelillo, and A. Prati, "Multi-object tracking using dominant sets," *IET Comput. Vis.*, vol. 10, pp. 289–298, 2016.
- [39] S. Vascon, E. Z. Mequanint, M. Cristani, H. Hung, M. Pelillo, and V. Murino, "Detecting conversational groups in images and sequences: A robust game-theoretic approach," *Comput. Vis. Image Understanding*, vol. 143, pp. 11–24, 2016.
- [40] R. Horst, P. Pardalos, and N. Van Thoai, *Introduction to Global Optimization*. Dordrecht/Boston/London: Kluwer Academic Publishers, 2000.
- [41] I. M. Bomze, "On standard quadratic optimization problems," *J. Global Optimization*, vol. 13, no. 4, pp. 369–387, 1998.
- [42] I. M. Bomze, "Evolution towards the maximum clique," *J. Global Optimization*, vol. 10, no. 2, pp. 143–164, 1997.
- [43] M. Pelillo, "Replicator dynamics in combinatorial optimization," in *Encyclopedia of Optimization*, 2nd Ed. New York, NY, USA: Springer US, 2009, pp. 3279–3291.
- [44] S. Todorovic and N. Ahuja, "Region-based hierarchical image matching," *Int. J. Comput. Vis.*, vol. 78, no. 1, pp. 47–66, 2008.
- [45] M. Pavan and M. Pelillo, "Dominant sets and hierarchical clustering," in *Proc. 9th IEEE Int. Conf. Comput. Vis.*, 2003, pp. 362–369.
- [46] E. Zemene and M. Pelillo, "Interactive image segmentation using constrained dominant sets," in *Proc. Eur. Conf. Comput. Vis.*, 2016, pp. 278–294.
- [47] A. Oliva and A. Torralba, "Modeling the shape of the scene: A holistic representation of the spatial envelope," *Int. J. Comput. Vis.*, vol. 42, no. 3, pp. 145–175, 2001.
- [48] K. Simonyan and A. Zisserman, "Very deep convolutional networks for large-scale image recognition," *CoRR*, vol. abs/1409.1556, 2014.
- [49] L. Zheng, S. Wang, L. Tian, F. He, Z. Liu, and Q. Tian, "Query-adaptive late fusion for image search and person re-identification," in *Proc. IEEE Conf. Comput. Vis. Pattern Recognit.*, 2015, pp. 1741–1750.
- [50] S. Zhang, M. Yang, T. Cour, K. Yu, and D. N. Metaxas, "Query specific rank fusion for image retrieval," *IEEE Trans. Pattern Anal. Mach. Intell.*, vol. 37, no. 4, pp. 803–815, Apr. 2015.
- [51] G. Toliás, R. Sircé, and H. Jégou, "Particular object retrieval with integral max-pooling of CNN activations," in *Proc. Int. Conf. Learning Representations*, 2016.
- [52] F. Radenovic, G. Toliás, and O. Chum, "CNN image retrieval learns from bow: Unsupervised fine-tuning with hard examples," in *Proc. 14th Eur. Conf. Comput. Vis.*, 2016, pp. 3–20.
- [53] D. M. Chen, et al., "City-scale landmark identification on mobile devices," in *Proc. IEEE Conf. Comput. Vis. Pattern Recognit.*, 2011, pp. 737–744.
- [54] G. Toliás, Y. S. Avrithis, and H. Jégou, "Image search with selective match kernels: Aggregation across single and multiple images," *Int. J. Comput. Vis.*, vol. 116, no. 3, pp. 247–261, 2016.

- [55] H. Jegou, M. Douze, and C. Schmid, "Product quantization for nearest neighbor search," *IEEE Trans. Pattern Anal. Mach. Intell.*, vol. 33, no. 1, pp. 117–128, Jan. 2011.



Eyasu Zemene received the BSc degree in electrical engineering from Jimma University, in 2007, he then worked at Ethio Telecom for 4 years till he joined CaFoscari University (October 2011) where he received the MSc degree in computer science, in June 2013. September 2013, he won a 1 year research fellow to work on Adversarial Learning at Pattern Recognition and Application lab of University of Cagliari. Since September 2014 he is working toward the PhD degree of CaFoscari University under the supervision of

Prof. Pelillo. Working towards his PhD he is trying to solve different computer vision and pattern recognition problems using theories and mathematical tools inherited from graph theory, optimization theory and game theory. Currently, he, as part of his PhD, is working as a research assistant at Center for Research in Computer Vision at University of Central Florida under the supervision of Dr. Mubarak Shah. His research interests include the areas of computer vision, pattern recognition, machine learning, graph theory and game theory.



Yonatan Tariku received the BSc degree in computer science from Arba Minch University, in 2007 and received the MSc degree (with Honor) in computer science, in 2014. He has worked 5 years with Ethio-telecom as senior programmer and later joined CaFoscari University of Venice. He is currently working toward the PhD degree at IUAV University of Venice starting from 2014. He is now a research assistant, towards his PhD, at Center for Research in Computer Vision at University of Central Florida. His research interests include multi-target tracking, segmentation, image and video geo-localization, game theoretic model, and graph theory.



Haroon Idrees received the BSc (Hons) degree in computer engineering from the Lahore University of Management Sciences, Pakistan, in 2007, and the PhD degree in computer science from the University of Central Florida, in 2014. He is a postdoctoral associate in the Center for Research in Computer Vision, University of Central Florida. He has published several papers in conferences and journals such as CVPR, ECCV, the *Journal of Image and Vision Computing*, and the *IEEE Transactions on Pattern Analysis and Machine*

Intelligence. His research interests include crowd analysis, object detection and tracking, wide area analysis, multi-camera and airborne surveillance, and multimedia content analysis.



Andrea Prati received the graduate degree in computer engineering from the University of Modena and Reggio Emilia, in 1998. He received the PhD degree in information engineering from the University of Modena and Reggio Emilia, in 2002. After some post-doc position with the University of Modena and Reggio Emilia, he was appointed as assistant professor in the Faculty of Engineering of Reggio Emilia (University of Modena and Reggio Emilia) from 2005 to 2011, and then as associate professor in the Department of Design

and Planning in Complex Environments of the University IUAV of Venice, Italy. In 2013 he has been promoted to full professorship, waiting for official hiring in the new position. In December 2015 he moved to the Department of Engineering and Architecture of the University of Parma. Author of 7 book chapters, 31 papers in international referred journals (including 9 papers published in IEEE Transactions) and more than 100 papers in proceedings of international conferences and workshops. He is senior member of the IEEE, fellow of the IAPR ("For contributions to low- and high-level algorithms for video surveillance"), and member of GIRPR.



Marcello Pelillo is full professor of computer science with CaFoscari University, in Venice, Italy, where he directs the European Centre for Living Technology (ECLT) and leads the Computer Vision and Pattern Recognition group. He held visiting research positions with Yale University, McGill University, the University of Vienna, York University (UK), the University College London, and the National ICT Australia (NICTA). He has published more than 200 technical papers in refereed journals, handbooks, and conference proceedings in the areas of pattern recognition, computer vision and machine learning.

He is general chair for ICCV 2017 and has served as program chair for several conferences and workshops (EMMCVPR, SIMBAD, S+SSPR, etc.). He serves (has served) on the Editorial Boards of the journals the *IEEE Transactions on Pattern Analysis and Machine Intelligence (PAMI)*, the *Pattern Recognition*, the *IET Computer Vision*, the *Frontiers in Computer Image Analysis*, the *Brain Informatics*, and serves on the Advisory Board of the *International Journal of Machine Learning and Cybernetics*. He is a fellow of the IEEE and a fellow of the IAPR.



Mubarak Shah the Trustee chair professor of computer science, is the founding director of the Center for Research in Computer Vision at the University of Central Florida (UCF). He is an editor of an international book series on video computing, editor-in-chief of *Machine Vision and Applications* journal, and an associate editor of *ACM Computing Surveys* journal. He was the program cochair of CVPR 2008, an associate editor of the *IEEE Transactions on Pattern Analysis and Machine Intelligence*, and a guest editor of

the special issue of the *International Journal of Computer Vision on Video Computing*. His research interests include video surveillance, visual tracking, human activity recognition, visual analysis of crowded scenes, video registration, UAV video analysis, and so on. He is an ACM distinguished speaker. He was an IEEE distinguished visitor speaker for 1997–2000 and received the IEEE Outstanding Engineering Educator Award in 1997. In 2006, he was awarded a Pegasus Professor Award, the highest award at UCF. He received the Harris Corporations Engineering Achievement Award in 1999, TOKTEN awards from UNDP in 1995, 1997, and 2000, Teaching Incentive Program Award in 1995 and 2003, Research Incentive Award in 2003 and 2009, Millionaires Club Awards in 2005 and 2006, University Distinguished Researcher Award in 2007, Honorable mention for the ICCV 2005 Where Am I? Challenge Problem, and was nominated for the Best Paper Award at the ACM Multimedia Conference in 2005. He is a fellow of the IEEE, AAAS, IAPR, and SPIE.

► For more information on this or any other computing topic, please visit our Digital Library at www.computer.org/publications/dlib.